

MLPruning: A Multilevel Structured Pruning Framework for Transformer-based Models

Zhewei Yao¹, Linjian Ma², Sheng Shen¹, Kurt Keutzer¹, Michael W. Mahoney¹
¹University of California, Berkeley, ²University of Illinois at Urbana-Champaign
 {zhewei, sheng.s, keutzer, mahoneymw}@berkeley.edu, lma16@illinois.edu

June 1, 2021

Abstract

Pruning is an effective method to reduce the memory footprint and computational cost associated with large natural language processing models. However, current approaches either only explore head pruning, which has a limited pruning ratio, or only focus on unstructured pruning, which has negligible effects on the real inference time and/or power consumption. To address these challenges, we develop a novel MultiLevel structured Pruning (MLPruning) framework, which uses three different levels of structured pruning: head pruning, row pruning, and block-wise sparse pruning. We propose using a learnable Top-k threshold, which employs an adaptive regularization to adjust the regularization magnitude adaptively, to select appropriate pruning ratios for different weight matrices. We also propose a two-step pipeline to combine block-wise pruning with head/row pruning to achieve high structured pruning ratios with minimum accuracy degradation. Our empirical results show that for BERT_{base}, with ~20% of remaining weights, MLPruning can achieve an accuracy that is comparable to the full model on QQP/MNLI/SQuAD, with up to ~3.69x speedup. Our framework has been open sourced [1].

1 Introduction

Since the development of self-attention models [43], the number of parameters for natural language processing (NLP) models has become much larger, e.g., BERT_{Large} (330M) [8], Megatron-LM (8.3B) [38], T5 (11B) [32], and GPT3 (170B) [4]. Although larger models tend to exhibit better generalization ability for downstream tasks, the inference time and associated power consumption become important bottlenecks to deploying those models on both cloud and edge devices.

One of the promising approaches for addressing the inference time and power consumption issues of these large models is pruning [36, 27, 44]. Most of the previous pruning work in NLP has focused on unstructured pruning [36, 7, 50, 31, 57], rather than structured pruning [27, 11]. Although unstructured pruning can reduce the number of weight parameters in the inference model, it is hard to get substantial speedups, since unstructured sparsity leads to sparse matrix multiplications (MatMul). These are typically memory bandwidth bound [5, 14] and hence have small performance advantages with moderate size sparsity. On the other hand, structured pruning can reduce the memory footprint, power consumption, and real inference time, but it usually cannot reach as high compression ratios as unstructured pruning.

Motivated by these issues, we propose a MultiLevel structured Pruning (MLPruning) framework, which takes into consideration different levels of model structure when pruning the model. The following are our contributions.

- We propose MLPruning, which consists of three different levels of structured pruning: (i) Head pruning (HPruning) for multi-head attention (MHA); (ii) Row pruning (RPruning) for general fully-connected layers; and (iii) block-wise sparsity pruning (BPruning) for all weight matrices. See § 3.1.

- We propose a learnable threshold for Top-k pruning, which adjusts the pruning ratio of different weight matrices based on an importance score. To control the regularization loss better, we design a novel adaptive regularization. The magnitude of the regularization loss is automatically adjusted to be large (small) when the current pruning ratio is far away (close to) the final ratio. See § 3.2.
- We propose a two-step pipeline to incorporate BPruning with HPruning and RPruning in a seamless way. Our results show that using BPruning on top of HPruning and RPruning can significantly reduce the accuracy degradation, while still achieving high speedup. See § 3.3.
- We benchmark our pruned model (with/without BPruning) based on the implementation on top of PyTorch [30]. In particular, we make use of the block-sparse MatMul kernel from Triton [42], and we show that block sparsity can reduce both memory footprint and inference time. See § 3.4.

Our empirical results demonstrate that MLPruning can reduce the model size of BERT_{base} by ~80%, while achieving minimal accuracy degradation on QQP/MNLI/SQuAD. In terms of speedup, our pruned QQP model with 14.19% of remaining weights and less than 1% performance degradation achieves up to 3.69x more throughput than its full-model counterpart. We also discuss in detail the effectiveness of our learnable threshold method, compared to a brute-force grid search method, the impact of head/row pruning on MHA, the impact of using different teacher models for BPruning, and the comparison between MLPruning and pure BPruning.

2 Related Work

Different approaches have been proposed to compress large pre-trained NLP models. These efforts can be generally categorized as follows: (i) knowledge distillation [21, 41, 35, 39]; (ii) quantization [3, 54, 37, 12, 53, 55, 2, 10]; (iii) new architecture design [40, 19, 23, 22, 45]; and (iv) pruning. Pruning can be broadly categorized into unstructured pruning [9, 24, 49, 29, 15, 36] and structured pruning [26, 16, 51, 25, 18, 56, 52, 27]. Here, we briefly discuss the related pruning work in NLP.

For unstructured pruning, [50, 7, 31] explore the lottery-ticket hypothesis [13] for transformer-based models; [57] shows that pruning is an alternative effective way to fine-tune pre-trained language models on downstream tasks; and [36] proposes so-called movement pruning, which considers the changes in weights during fine-tuning for a better pruning strategy, and which achieves significant accuracy improvements in high sparsity regimes. However, none of these shows inference time speedup in practice.

For structured pruning, [11, 34] uses LayerDrop to train the model and observes that small/efficient models can be extracted from the pre-trained model; [46] uses a low-rank factorization of the weight matrix and adaptively removes rank-1 components during training; and [27] tests head drop for multi-head attention and concludes that a large percentage of attention heads can be removed during inference without significantly affecting the performance. Similar to [27], MLPruning also uses head pruning; however, MLPruning jointly removes heads and rows at the same time. Also, MLPruning prunes all heads during the training, while [27] does iterative pruning for high head pruning ratios. Finally, [28, 47, 6] study row and block-wise pruning for LSTM [17]. However, none of them considers different sparse levels together or works on transformer-based models; and the algorithms underlying [28, 47, 6] are very different than the pruning algorithm used in MLPruning.

3 Methodology

The basic ingredients of transformer-based models are multi-headed attention (MHA) and fully-connected (FC) layers. Here, we briefly review the structures of MHA.¹ In MHA, H independently parameterized

¹For simplicity, we use the encoder block in BERT as an example, and we ignore all bias terms, non-linear operators, and residual connections.

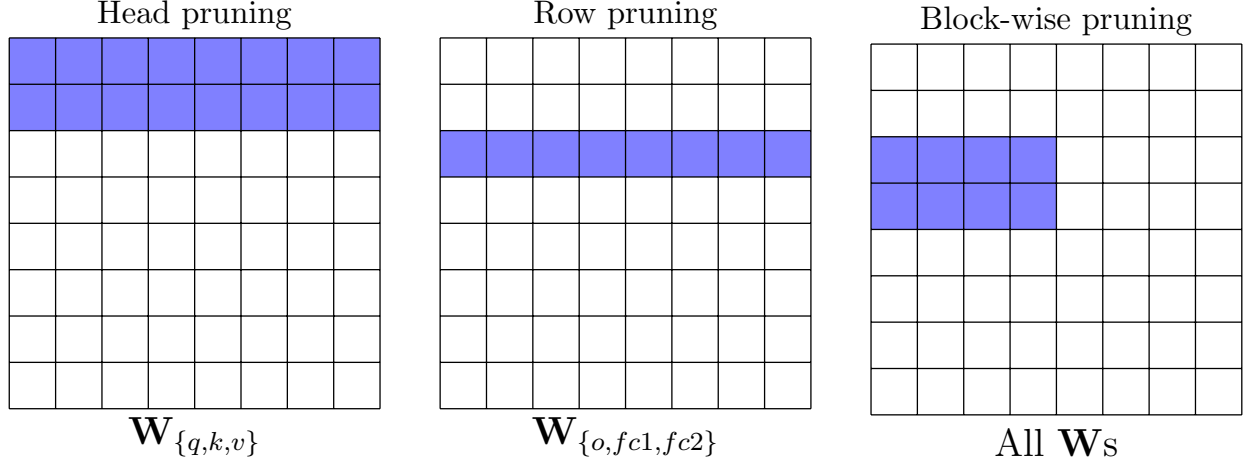


Figure 1: The illustration of different levels of structured pruning, i.e., head pruning (HPruning), row pruning (RPruning), and block-wise pruning (BPruning). Blue colored cells represent the pruned weights.

attention heads are applied to obtain the final result:

$$\text{MHA}(\mathbf{x}, \mathbf{q}) = \sum_{h=1}^H \text{Att}_{\mathbf{w}_{q,h}, \mathbf{w}_{k,h}, \mathbf{w}_{v,h}, \mathbf{w}_{o,h}}(\mathbf{x}, \mathbf{q}) \equiv \sum_{h=1}^H \text{Att}_h(\mathbf{x}, \mathbf{q}), \quad (1a)$$

$$\text{Att}_{\mathbf{w}_{q,h}, \mathbf{w}_{k,h}, \mathbf{w}_{v,h}, \mathbf{w}_{o,h}}(\mathbf{x}, \mathbf{q}) = \mathbf{W}_{o,h} \sum_{i=1}^n \alpha_i \mathbf{W}_{v,h} \mathbf{x}_i \quad \text{and} \quad \alpha_i = \text{softmax}\left(\frac{\mathbf{q}^T \mathbf{W}_{q,h}^T \mathbf{W}_{k,h} \mathbf{x}}{\sqrt{d}}\right), \quad (1b)$$

where $\mathbf{x} = [\mathbf{x}_1, \dots, \mathbf{x}_n] \in \mathbb{R}^{n \times d}$ is the input sequence feature map, $\mathbf{W}_{\{q,k,v\},h} \in \mathbb{R}^{d_h \times d}$ ($d_h = d/H$) and $\mathbf{W}_{o,h} \in \mathbb{R}^{d \times d_h}$ are weight matrices, and $\mathbf{q} \in \mathbb{R}^d$ is the query vector. To allow different attention heads to interact with each other, transformers apply two FC layers over the MHA's output, i.e.,

$$\text{FC}_2(\text{FC}_1(\text{MHA}(\mathbf{x}, \mathbf{q}))) = \mathbf{W}_{fc2} \mathbf{W}_{fc1} \text{MHA}(\mathbf{x}, \mathbf{q}), \quad (2)$$

where $\mathbf{W}_{fc1} \in \mathbb{R}^{4d \times d}$ and $\mathbf{W}_{fc2} \in \mathbb{R}^{d \times 4d}$.

3.1 The Multilevel Structured Pruning Framework

Let $\mathbf{W} \in \mathbb{R}^{d \times d}$ refer to a generic weight matrix (\mathbf{W} could be a non-square matrix/tensor), \mathbf{S} refer to the associated importance score matrix of \mathbf{W} with the proper shape, and \mathbf{M} refer to the mask matrix of \mathbf{W} with the same shape as \mathbf{S} . For inference, the weight matrix \mathbf{W} is masked by \mathbf{M} . (See Appendix A for masking details.)

To compute \mathbf{M} , we use the Top-k threshold of weights by the importance of \mathbf{S} , i.e.,

$$\mathbf{M} = \text{Top}_k(\mathbf{S}), \quad \text{where} \quad \text{Top}_k(\mathbf{S}_{i,j}) = \begin{cases} 1 & \text{if } \mathbf{S}_{i,j} \text{ is in the top-k region,} \\ 0 & \text{otherwise.} \end{cases} \quad (3)$$

Different importance score matrices \mathbf{S} have been proposed; and here we use a variant of the learnable \mathbf{S} from [58], where \mathbf{S} is updated during training. Different than [58], which applies the technique to unstructured pruning, we extend this algorithm to structured pruning. In addition, instead of fixing the thresholds for all weight matrices, one of our contributions (see § 3.2) is that we introduce a novel algorithm for a learnable threshold for Top-k selection.

We discuss the three main different levels (i.e., head, row, and block-wise sparse pruning) of structured pruning as follows. By grouping different parts in \mathbf{W} , we can get different structured pruning mechanisms.

Head Pruning for Attention (HPruning). We use the same head pruning definition as [27], i.e., $\text{MHA} = \sum_{h=1}^H \xi_h \text{Att}_h(\mathbf{x}, \mathbf{q})$, where $\xi_h \in \{0, 1\}$ is a binary variable. HPruning is applied on the matrix $\mathbf{W}_{\{q,k,v\}} \in \mathbb{R}^{(Hd_h) \times d}$, which stacks all attention weight matrices. In this setting, $\mathbf{S} \in \mathbb{R}^H$ and $\mathbf{M} \in \mathbb{R}^H$. When $\mathbf{M}[i] = 0$, the i -th head of MHA, is pruned, i.e., $\mathbf{W}_{\{q,k,v\}}[id_h : (i+1)d_h, :] \equiv \mathbf{W}_{\{q,k,v\},i} = 0$. (Here, we use Numpy/PyTorch matrix index notation.) HPruning is illustrated in the left panel of Figure 1.

Row Pruning for FC (RPruning). For the remaining weight matrices, i.e., $\mathbf{W}_{\{o,fc1,fc2\}}$ (\mathbf{W}_o is the stacked matrix of all $\mathbf{W}_{o,h}$), we can apply row pruning, which indicates that an entire row of the weight matrix is removed. RPruning is illustrated in the middle panel of Figure 1. For example, here $\mathbf{S} \in \mathbb{R}^d$ and $\mathbf{M} \in \mathbb{R}^d$ for \mathbf{W}_o .

Block-wise Pruning (BPruning). After HPruning and RPruning, the resulting matrix (e.g., \mathbf{W}_{fc1}) becomes much smaller than the original one. However, aggressively applying HPruning and/or RPruning usually leads to significant accuracy degradation (see § 4.2). To achieve higher compression ratios, we use block-wise pruning to further prune the resulting matrix after head/row pruning. Consider an output matrix after head/row pruning as $\mathbf{W} \in \mathbb{R}^{m \times n}$, where $m = ar$ and $n = bc$, and a, b are integer numbers, r and c are the numbers of rows and columns of each block, respectively. For block-wise pruning, $\mathbf{S} \in \mathbb{R}^{a \times b}$ and $\mathbf{M} \in \mathbb{R}^{a \times b}$ for \mathbf{W} . When $\mathbf{M}[i, j] = 0$, we set all elements in the (i, j) -th block of \mathbf{W} as 0. This is illustrated in the right panel of Figure 1.

By combining different pruning levels together, we have the following two multi-level structured pruning methods.

HPruning+RPruning (MLPruning-Partial). As a result of HPruning and RPruning, some corresponding columns of weight matrices ($\mathbf{W}_{\{o,fc2\}}$) can also be pruned since the outputs of MHA and FC1 have fewer dimensions, as compared to their full counterpart. (For other weight matrices, this cannot be applied due to the residual connection.) We refer to this method as MLPruning-Partial and illustrate this in Figure B.1.

HPruning+RPruning+BPruning (MLPruning). As a result of all three pruning methods, all weight matrices become smaller as compared to the original full counterparts and they are also block-wise sparse. We refer to this method as MLPruning and illustrate this in Figure B.2.

3.2 Learnable Top-k Selection and Adaptive Regularization for Pruning

In [58, 36], the Top- k threshold is fixed for all weight matrices. However, different weight matrices have different tolerances/sensitivities to pruning, meaning that a high pruning ratio needs to be applied for insensitive layers, and vice versa. Another disadvantage of using a fixed target pruning ratio is that the thresholds are hard to decide when applying hybrid pruning techniques. For example, when we apply HPruning and RPruning together, which one should be dominant is unclear from [58, 36].

In order to resolve these issues, we propose an algorithm to learn the Top- k threshold. Suppose the learnable threshold is σ of a weight matrix \mathbf{W} . Then the parameter k is defined as

$$k = \text{Sigmoid}(\sigma), \quad (4)$$

where the Sigmoid function is used to map σ to be in the range of $(0, 1)$. However, directly applying this will tend to make k always close to 1, since the model prefers no pruning. Therefore, we introduce a regularization term to compensate for this.

For the i -th layer, suppose that the head threshold of $\mathbf{W}_{\{q,k,v\}}$ is k_h^i , the row threshold of \mathbf{W}_o is k_o^i , and the row thresholds of $\mathbf{W}_{fc1}/\mathbf{W}_{fc2}$ are k_f^i/k_s^i .² Then the number of remaining parameters of the i -th layer is

$$N^i = 3k_h N_h + k_h k_o N_o + k_f N_f + k_f k_s N_s, \quad (5)$$

²For simplicity, we will drop the superscript when there is no confusion.

where N_h , N_o , N_f and N_s are the number of parameters of $\mathbf{W}_{\{q,k,v\}}$, \mathbf{W}_o , \mathbf{W}_{fc1} , and \mathbf{W}_{fc2} of the layer, respectively. For the entire encoder, the remaining parameter ratio can be computed as

$$R = \left(\sum_{i=1}^L N^i \right) / (L(3N_h + N_o + N_f + N_s)). \quad (6)$$

Suppose that our target ratio is R_{target} . We propose the following regularization loss,

$$\mathcal{L}_{reg} = \begin{cases} (R - R_{target})^2 & R \geq R_{target}, \\ 0 & \text{else.} \end{cases} \quad (7)$$

Given this, we then rewrite the training objective as

$$\mathcal{L} = \mathcal{L}_{obj} + \lambda_{reg} \mathcal{L}_{reg}, \quad (8)$$

where \mathcal{L}_{obj} is the original training loss and λ_{reg} is the regularization magnitude.

Generally, for different pruning regularization methods (e.g., L_1/L_0 regularization), λ_{reg} needs to be carefully tuned for both initial values and its schedule [36]. To resolve this tuning issue, we propose an adaptive formula to choose the value of λ_{reg} ,

$$\lambda_{reg} = \max \left\{ \lambda_{max} \frac{\mathcal{L}_{reg}}{(1 - R_{target})^2}, \lambda_{min} \right\}, \quad (9)$$

where $\lambda_{max}/\lambda_{min}$ are pre-chosen hyperparameters.³ (We have found that our results are not sensitive to the choice of these hyperparameters; and we have kept them the same on each dataset in all of our results.) The idea of Eq. 9 is that when R is far away from the R_{target} , λ_{reg} is chosen that is close to λ_{max} (when $R = 1$, it is indeed λ_{max}) so that we can have a strong regularization effect; and when R is close to R_{target} , then we do not have to stress the regularization term (Eq. 7) too much.

3.3 Two-step Pipeline

If BPruning is performed concurrently with MLPruning-Partial, there will be sparse blocks overlapping with head/row pruning. This not only causes the measurement of the remaining parameters to be hard to compute, but it also makes the hardware deployment challenging since the hardware needs to deal with nonuniform sparse block sizes, even within a single weight matrix.

Therefore, in our experiments, we propose a two-step pipeline for MLPruning. In the first step, we only do HPruning and RPruning over the model. In the second step, we remove those pruned heads/rows from the model, and then we apply BPruning. For BPruning, we use the same method as mentioned in § 3.2. The only difference is that for \mathbf{W}_o and \mathbf{W}_{fc2} , there is no column pruning contribution from MHA or FC₁ anymore, so that Eq. 5 needs to be modified as

$$N^i = k_{q,r}N_{q,r} + k_{k,r}N_{k,r} + k_{v,r}N_{v,r} + k_{o,r}N_{o,r} + k_{f,r}N_{f,r} + k_{s,r}N_{v,r}, \quad (10)$$

where $k_{*,r}$ is the threshold of W_* , and $N_{*,r}$ is the current number of parameters of W_* after MLPruning-Partial. Moreover, we add padding to the input matrices for BPruning when the row/column size is not divisible by the block size. For example, if the matrix has size 100x768 (with original size 768x768) after RPruning and the block size is 16x16, we use the important score \mathbf{S} to get another 12 rows to pad the matrix to be in the size of 112x768 so that we can successfully partition the weight matrix with block size 16x16.

3.4 Hardware Deployment for Block Sparsity

Although fewer parameters can help reducing the memory footprint, it alone is not a good indicator of efficiency, e.g., inference time and power consumption. Compared to the general sparsity pattern, block sparsity allows for a higher degree of parallelizability. Optimized block-sparse kernels can bring substantial

³Note that \mathcal{L}_{reg} here is just used as a scalar value, which does not affect the computation of gradient. For instance, in PyTorch/TensorFlow, we need to detach it from the computational graph.

Table 1: Performance of MLPruning-Partial on different datasets. For the last performance column, we report the mean of F1 and accuracy score on QQP, the accuracy for MNLI-M/MM on MNLI, and the exact match (EM) and F1 on SQuAD.

Dataset	Remaining Weight %	Remaining Heads ($\mathbf{W}_{\{q,k,v\}}$) %	Remaining FC Weight %			Performance
			\mathbf{W}_o	\mathbf{W}_{fc1}	\mathbf{W}_{fc2}	
QQP	100	100	100	100	100	89.91
	44.27	61.81	42.82	54.16	21.49	89.22
	39.87	61.81	35.90	38.53	25.65	89.06
	28.82	54.17	34.88	19.22	17.78	88.67
	22.12	54.17	34.02	8.58	8.53	88.24
MNLI	100	100	100	100	100	84.47/84.83
	48.54	77.08	51.98	42.95	31.76	83.51/84.03
	41.40	69.44	51.31	29.83	29.37	83.25/83.81
	30.91	54.17	43.23	20.75	20.43	82.53/82.96
	21.78	46.53	35.04	10.82	10.73	81.81/81.99
SQuAD	100	100	100	100	100	80.92/88.52
	60.45	77.78	73.37	54.91	49.38	81.02/88.30
	51.33	77.08	72.20	41.56	36.47	80.26/87.91
	40.72	67.36	60.85	28.24	28.04	79.35/86.98
	31.49	68.75	60.73	13.79	13.78	78.62/86.66
	21.98	63.19	54.74	2.66	2.64	74.60/83.81

speedups compared to dense kernels with moderate sparsity (more than 70%⁴). In our experiments, we leverage the optimized block sparse MatMul kernel provided by Triton [42], a compiler for tiled neural network computation on GPUs, to accelerate our pruned model after BPruning.

We evaluate the performance with block sizes 16x16 and 32x32 on a T4 GPU. Larger block sizes result in slightly larger accuracy degradation, while smaller block sizes (e.g., 4x4 or 8x8) cannot be efficiently deployed on GPU tensor cores and are not supported by Triton. However, those small block sizes can definitely be used for other accelerators, e.g., CPU and FPGA. Also, note that our BPruning can also be used with non-square block sizes, e.g., 16x32.

For each linear layer, we use the block sparse MatMul kernel provided by Triton if the sparsity is higher than a pre-defined threshold, and we use the dense MatMul kernel in PyTorch otherwise. The threshold is set as 0.8 when the block size is 16x16 and 0.6 when the block size is 32x32; and the numbers are picked so that block sparse kernels offer real speedups for most of the MatMul configurations.

4 Results

4.1 Experimental Setup

We apply MLPruning with task-specific pruning for BERT_{base} [8] on three monolingual (English) tasks: question answer (SQuAD v1.1) [33]; sentence similarity (QQP) [20]; and natural language inference (MNLI) [48]. For SQuAD/QQP/MNLI, there are 88K, 364K, 392K training examples.

For all tasks, we perform distillation to boost the performance. In particular, we simplify the distillation pipeline from [21]. Rather than using a two-step task-specific distillation (i.e., intermediate layer distillation

⁴The data comes from <https://developer.nvidia.com/blog/accelerating-matrix-multiplication-with-block-sparse-format-and-nvidia-tensor-cores/>.

followed by prediction layer distillation), we directly combine these two steps together, i.e., we use

$$\mathcal{L} = (1 - \alpha)\mathcal{L}_{CE} + \alpha(\mathcal{L}_{DS} + \mathcal{L}_{MHA} + \mathcal{L}_{hidden}) + \lambda_{reg}\mathcal{L}_{reg}. \quad (11)$$

Here, \mathcal{L}_{DS} is the KL-divergence between the predictions of the student and the teacher, \mathcal{L}_{MHA} is the attention alignment loss, \mathcal{L}_{hidden} is the hidden feature (the output of \mathbf{W}_o with residual connection) alignment loss, and α is the hyperparameter that balances the importance of the cross-entropy loss and the distillation loss. For MLPruning-Partial, we use the full model as the teacher. For BPruning after MLPruning-Partial, we use the pruned model after MLPruning-Partial as the teacher. For all of our results, we choose $\alpha = 0.9$. (One might be able to improve the results further with more careful hyperparameter tuning and more sophisticated distillation methods.) For more training details, see Appendix C.

4.2 Results of MLPruning-Partial

We start with MLPruning-Partial with different pruning ratios on different datasets. Results are shown in Table 1. As can be seen, with 39.87/41.40/51.33% of remaining weights, MLPruning-Partial can achieve ~1% performance degradation on QQP/MNLI/SQuAD. Furthermore, reducing the number of parameters generally results in a large accuracy drop on all datasets. However, for a relatively simple task, e.g., QQP, the performance degradation is smaller than other relatively harder tasks (MNLI/SQuAD). In particular, for ~20% of remaining weights, the performance degradation of QQP is ~1.7, which is much smaller than ~6.3 (EM) or ~4.7 (F1) of SQuAD.

We also report the number of remaining parameters of each type of weight matrices in Table 1. Note that for MHA, the $\mathbf{W}_{\{q,k,v\}}$ are correlated with each other, and so we combine the results of them into one column. There are several interesting findings: (i) $\mathbf{W}_{\{q,k,v\}}$ are less pruned than other matrices, particularly for high pruning ratio (i.e., fewer remaining weights); (ii) the row pruning ratio of \mathbf{W}_o is no larger than 50%; and although the remaining weights of \mathbf{W}_o are less than 35% (e.g., last row on QQP), the majority parameter reduction is contributed by column pruning (Figure B.1); (iii) the row pruning ratio of \mathbf{W}_{fc1} is extremely high for high pruning ratios; and (iv) there is almost no row pruning applied to \mathbf{W}_{fc2} . Similar to the observation (ii), almost all weight reduction of \mathbf{W}_{fc2} comes from the column pruning which is related to \mathbf{W}_{fc1} .

4.3 Results of MLPruning

Here, we discuss the results of BPruning built on top of MLPruning-Partial (i.e., MLPruning) with various block sparsity levels on QQP/MNLI/SQuAD. In particular, the models used for BPruning are the ones with 44.27%, 48.54%, and 60.45% of remaining weights on QQP, MNLI, and SQuAD, as shown in Table 1, respectively.

The results of MLPruning are presented in Table 2. For each dataset, there are three sections. The first section shows results for MLPruning-Partial. In the second/third section of rows, we show results for MLPruning with block size 16x16/32x32. Notice that using BPruning along with MLPruning-Partial can achieve better performance, compared to using just MLPruning-Partial. In particular, on SQuAD, with ~20% of remaining weights, MLPruning achieves 0.82/0.64 better F1 score than MLPruning-Partial with block size 16x16/32x32. Additionally, note that smaller block size generally results in better performance. For more block size settings and block sparsity settings, see Appendix D.

Table 2 also shows results for the block density, which is the percentage of dense/unpruned blocks in the matrix, for each type of weight matrix. Again, some interesting findings can be seen: (i) \mathbf{W}_k is generally less pruned than all other matrices; (ii) $\mathbf{W}_{fc1,fc2}$ are the most heavily pruned weight matrices, particularly for high sparsity levels; (iii) more \mathbf{W}_o parameters will remain when a high pruning ratio is applied for the entire model; and (iv) the correlations between the sparsity of $\mathbf{W}_q/\mathbf{W}_v$ and \mathbf{W}_k have very different behaviors, depending on whether the task is text classification or question answering. For instance, when the task is text classification, i.e., QQP/MNLI, the sparsity of \mathbf{W}_q has the same trend as \mathbf{W}_k , which usually has more weight left as compared to \mathbf{W}_v . However, for question answering, i.e., SQuAD, the opposite happens. This may be caused by the longer sequences in SQuAD and/or other difference in the problem structure.

Table 2: Performance of MLPruning on different datasets. For the last performance column, we report the mean of F1 and accuracy score on QQP, the accuracy for MNLI-M/MNLI-MM on MNLI, and the exact match (EM) and F1 on SQuAD. Here we only report two pruning ratios for each block size. See Table D.1 for all the results.

Dataset	Block Size	Remaining Weight %	Block Density %						Performance
			\mathbf{W}_q	\mathbf{W}_k	\mathbf{W}_v	\mathbf{W}_o	\mathbf{W}_{fc1}	\mathbf{W}_{fc2}	
QQP	–	44.27	100	100	100	100	100	100	89.22
	–	22.12	100	100	100	100	100	100	88.24
	16x16	34.76	90.48	95.28	59.98	33.45	75.81	97.23	89.09
	16x16	11.97	56.33	56.35	41.18	60.30	4.49	13.49	88.46
	32x32	34.75	87.97	95.58	64.42	38.35	83.12	72.88	88.99
	32x32	14.28	71.14	62.27	51.40	64.70	6.39	16.01	88.56
MNLI	–	48.54	100	100	100	100	100	100	83.51/84.03
	–	21.78	100	100	100	100	100	100	81.81/81.99
	16x16	37.74	99.78	99.69	63.76	52.57	89.29	54.48	82.57/83.12
	16x16	20.31	71.01	71.75	47.44	69.93	18.28	23.06	81.71/82.59
	32x32	36.89	92.23	99.77	59.53	53.61	88.23	53.35	82.51/83.19
	32x32	20.40	71.00	71.67	47.45	69.93	18.34	23.05	81.71/82.49
SQuAD	–	60.45	100	100	100	100	100	100	81.02/88.30
	–	21.98	100	100	100	100	100	100	74.60/83.81
	16x16	48.30	95.52	98.15	78.97	71.69	81.94	66.84	80.83/88.11
	16x16	20.97	48.53	80.38	80.53	90.58	4.85	4.22	75.70/84.63
	32x32	45.13	93.51	97.25	77.32	70.52	70.20	62.50	80.56/87.85
	32x32	20.47	50.17	80.59	80.68	79.93	4.94	4.26	75.49/84.45

4.4 Real Hardware Deployment

We show the speedups of our methods compared to the baseline (full model) on a T4 GPU in Table 3. As can be seen, for larger batch size and/or longer sequence length, both MLPruning-Partial and MLPruning can achieve significant speedups, compared to the full model counterpart. In particular, for MLPruning-Partial, while still achieving 89.06% accuracy (within 1% lower than baseline), it can increase the throughput by 1.71x with batch size 1 and sequence length 512, or by 2.21x with batch size 32 and sequence length 128. For MLPruning, large speedups (up to 3.69x) are achieved when the block size is 16x16, batch size is 32, and the accuracy is 88.46% (within 1.5% accuracy degradation). In general, larger sparsity and larger block size (32x32) offer larger speedups.

One interesting finding here is that when batch size is 1 and sequence length is 128, there is no speedup for MLPruning at all, and the sparse kernel is actually slower than its dense counterpart. The small batch size and short sequence length mean that the input matrices to MatMul kernels have small sizes. This means that the GEMM floating point operations per second (flop/s) will decrease when the entire matrix size decreases. Since block sparse MatMul kernels internally call smaller-sized GEMM, their flop/s are much smaller than the large dense kernels. In this case, the computational cost advantage cannot make up for the flop/s slow down, making the block sparse kernels inefficient.

5 Additional Discussion

Learned Threshold versus Hard Threshold. To show the effectiveness of our learned threshold, we compare the performance of MLPruning-Partial to uniform hard threshold on QQP/MNLI. In particular, for

Table 3: Speedup of different models trained on QQP with various settings. The second row shows the percents of remaining weights, and the third row shows the average of accuracy and F1 score. Here, we abbreviate Batch Size as “Batch”, Sequence Length as “Seq”, Block Size as “BS”. We report the relative speedup for all models, and we report the inference throughput (sentences per second) of the full model in the parenthesis.

Batch/Seq	Full Model	MLPruning-Partial				MLPruning (BS 16x16)				MLPruning (BS 32x32)		
	100%	44.27%	39.87%	28.82%	22.12%	34.76%	18.55%	14.19%	11.97%	34.75%	18.73%	14.28%
	89.91	89.22	89.06	88.67	88.24	89.09	89.02	89.01	88.46	88.99	89.01	88.56
1/128	1.0 (62.8)	1.13	1.11	1.15	1.16	1.15	0.92	0.89	0.83	1.06	0.90	0.89
32/128	1.0 (152.7)	2.03	2.21	2.84	3.36	2.04	2.32	2.73	3.69	2.09	2.93	3.23
1/256	1.0 (51.5)	1.32	1.30	1.34	1.36	1.28	1.07	1.05	0.96	1.19	1.12	1.03
32/256	1.0 (72.0)	2.05	2.20	2.81	3.31	2.02	2.28	2.65	3.56	2.07	2.83	3.13
1/384	1.0 (37.5)	1.48	1.52	1.65	1.73	1.49	1.31	1.32	1.29	1.46	1.42	1.35
32/384	1.0 (45.0)	2.00	2.16	2.73	3.19	1.94	2.22	2.54	3.35	2.02	2.69	2.99
1/512	1.0 (28.7)	1.62	1.71	1.89	2.01	1.62	1.50	1.53	1.56	1.59	1.64	1.60
32/512	1.0 (32.0)	1.96	2.11	2.63	2.98	1.87	2.19	2.46	3.19	1.94	2.60	2.86

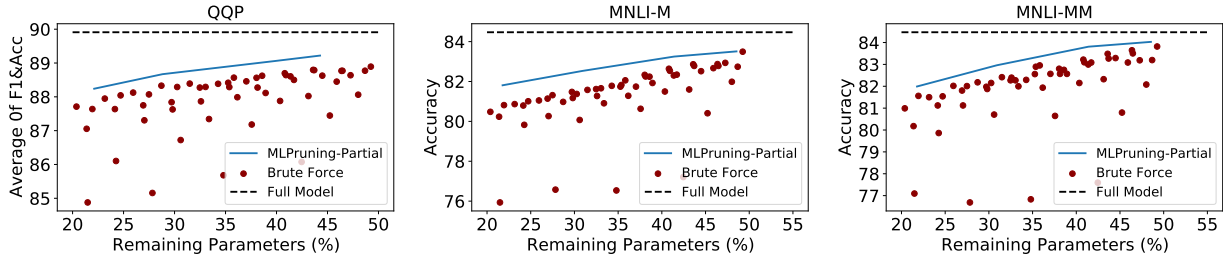


Figure 2: Comparison between our learnable threshold (§ 3.2) and brute-force search for different head/row pruning ratios on QQP/MNLI-M/MNLI-MM. See Appendix E for all brute force results.

hard threshold, we set a uniform head pruning ratio for all $\mathbf{W}_{\{q,k,v\}}$ and uniform row pruning ratio for all $\mathbf{W}_{\{o,fc1,fc2\}}$, and we use brute-force grid search to get all possible configurations. See Appendix E for more details. Results are shown in Figure 2. As can be seen, for both QQP/MNLI, our learnable threshold method achieves better accuracy than grid search.

One Full Head is Better than Two Half Heads. Although we use HPruning for $\mathbf{W}_{\{q,k,v\}}$, it is possible to use RPruning as well. However, we find out that for MHA, HPruning is more efficient than RPruning. That is to say, with similar pruning ratios, HPruning can achieve higher accuracy than RPruning. We conduct experiments for those two pruning strategies on QQP, and the results are shown in Table 4. Note that $\mathbf{W}_{\{fc1,fc2\}}$ are unpruned. As can be seen, HPruning can consistently achieve better performance on all cases.

Different Teacher Models for BPruning. Different teacher models can be used for BPruning after MLPruning-Partial, including the original full model and the pruned model after MLPruning-Partial. Here, we study the accuracy difference by using those two different types of teacher models. In particular, when we use the full model as the teacher, since the model used for BPruning has fewer heads in MHA, we have to remove the attention loss from Eq. 11 for distillation. Results are shown in Table 5. As can be seen, using the pruned model after MLPruning-Partial as the teacher can achieve better accuracy across different pruning ratios and different sparse block sizes. In particular, for high pruning ratio (<20% of remaining weights), using MLPruning-Partial as the teacher has much better accuracy than using the full model.

Table 4: Comparison between using RPruning and using HPruning for MHA. We report the mean of F1 and accuracy on QQP. Here, only the MHAs are pruned, i.e., FC_1 and FC_2 are in the full format. Also, the percentage reported in the first row are the remaining weights of MHA.

Method	92%	83%	75%	67%	58%	50%	42%	33%	25%	17%	8%
RPruning	89.73	89.62	89.51	89.41	89.17	88.70	88.68	88.77	88.33	87.93	86.97
HPruning	89.88	89.95	89.84	89.55	89.32	89.31	89.24	89.21	88.79	88.53	87.01

Table 5: Performance of different teachers for BPruning after MLPruning-Partial on QQP.

Teacher	Block Size	Remaining Parameters %	Average of F1&Acc
MLPruning-Partial Model	4x4	35.51	89.36
Full Model	4x4	35.57	89.34
MLPruning-Partial Model	4x4	14.13	89.10
Full Model	4x4	18.55	88.65
MLPruning-Partial Model	8x8	35.54	89.22
Full Model	8x8	35.58	89.09
MLPruning-Partial Model	8x8	14.15	89.02
Full Model	8x8	18.57	88.81
MLPruning-Partial Model	16x16	34.76	89.09
Full Model	16x16	34.76	89.07
MLPruning-Partial Model	16x16	14.19	89.01
Full Model	16x16	18.62	88.69
MLPruning-Partial Model	32x32	34.75	88.99
Full Model	32x32	35.86	88.81
MLPruning-Partial Model	32x32	14.28	88.56
Full Model	32x32	18.74	88.43

Comparison with Pure BPruning. One extreme case of our MLPruning is only using BPruning for all weight matrices instead of using multi-level structured pruning. This has several drawbacks: (i) there is almost no column pruning for $\mathbf{W}_{\{o,fc2\}}$ as shown in Figure B.1 and Eq. 5, since column pruning is contributed from the head/row pruning of the previous matrices; and this makes the high pruning ratio more challenging; (ii) for MHA, the computation of Softmax (α_i) and the following $\alpha_i \mathbf{W}_{v,h}$ in Eq. 1b can hardly be reduced; and (iii) it may result in less speedup, compared to MLPruning.

As to the first drawback, we find that pure BPruning actually leads to sub-optimal performance as compared to our MLPruning. Results for QQP/MNLI are shown in Figure 3. Note that for pure BPruning, we still use our learnable threshold with adaptive regularization, and we use the full model as the teacher for distillation. As can be seen, the performance of pure BPruning is significantly worse than that of MLPruning. In particular, for higher pruning ratios, the gap between pure BPruning and MLPruning becomes larger.

6 Conclusions

In this work, we present MLPruning, a multilevel structured pruning framework for transformer-based models. To select the pruning ratios for different weight matrices, we propose a learnable threshold with adaptive regularization to adjust the pruning ratio for (in-)sensitive layers. Moreover, we use a two-step pipeline to combine seamlessly BPruning with head/row pruning. We show that MLPruning can achieve performance comparable to the full model, while reaching extremely high structured pruning ratios. We also directly deploy the pruned models and measured the end-to-end inference throughput, showing that those pruned models can achieve up to $3.69\times$ speedup on a Tesla T4 GPU than the full model counterpart. Our analysis

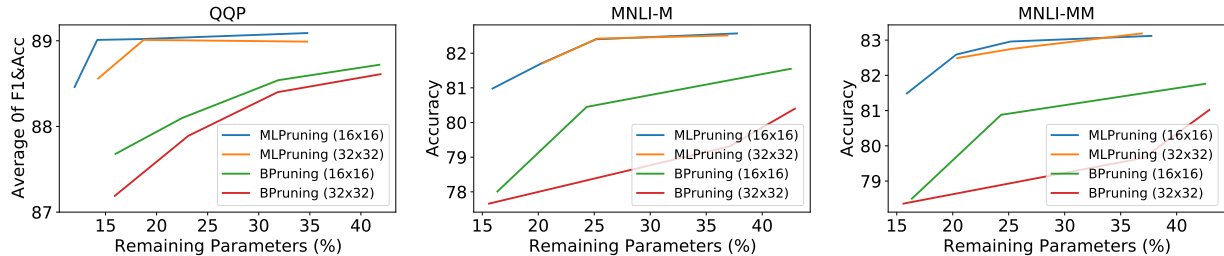


Figure 3: Comparison between MLPruning with pure BPruning.

shows that different components used in MLPruning are necessary to achieve high performance with high compression ratios.

Acknowledgments

This work was supported by a gracious fund from Intel, Samsung, and Facebook. We are also grateful for a gracious support from Google, and Amazon AWS. MWM would also like to acknowledge DARPA, NSF, and ONR for providing partial support of this work.

References

- [1] <https://github.com/yaozhewei/mlpruning.git>, May 2021.
- [2] Haoli Bai, Wei Zhang, Lu Hou, Lifeng Shang, Jing Jin, Xin Jiang, Qun Liu, Michael Lyu, and Irwin King. BinaryBERT: Pushing the limit of BERT quantization. *arXiv preprint arXiv:2012.15701*, 2020.
- [3] Aishwarya Bhandare, Vamsi Sripathi, Deepthi Karkada, Vivek Menon, Sun Choi, Kushal Datta, and Vikram Saletore. Efficient 8-bit quantization of transformer neural machine language translation model. *arXiv preprint arXiv:1906.00532*, 2019.
- [4] Tom B Brown, Benjamin Mann, Nick Ryder, Melanie Subbiah, Jared Kaplan, Prafulla Dhariwal, Arvind Neelakantan, Pranav Shyam, Girish Sastry, Amanda Askell, et al. Language models are few-shot learners. *arXiv preprint arXiv:2005.14165*, 2020.
- [5] Aydin Buluc and John R Gilbert. Challenges and advances in parallel sparse matrix-matrix multiplication. In *2008 37th International Conference on Parallel Processing*, pages 503–510. IEEE, 2008.
- [6] Shijie Cao, Chen Zhang, Zhuliang Yao, Wencong Xiao, Lanshun Nie, Dechen Zhan, Yunxin Liu, Ming Wu, and Lintao Zhang. Efficient and effective sparse lstm on fpga with bank-balanced sparsity. In *Proceedings of the 2019 ACM/SIGDA International Symposium on Field-Programmable Gate Arrays*, pages 63–72, 2019.
- [7] Tianlong Chen, Jonathan Frankle, Shiyu Chang, Sijia Liu, Yang Zhang, Zhangyang Wang, and Michael Carbin. The lottery ticket hypothesis for pre-trained BERT networks. *arXiv preprint arXiv:2007.12223*, 2020.
- [8] Jacob Devlin, Ming-Wei Chang, Kenton Lee, and Kristina Toutanova. BERT: Pre-training of deep bidirectional transformers for language understanding. In *NAACL-HLT*, 2019.
- [9] Xin Dong, Shangyu Chen, and Sinno Pan. Learning to prune deep neural networks via layer-wise optimal brain surgeon. In *Advances in Neural Information Processing Systems*, pages 4857–4867, 2017.

- [10] Steven K Esser, Jeffrey L McKinstry, Deepika Bablani, Rathinakumar Appuswamy, and Dharmendra S Modha. Learned step size quantization. *arXiv preprint arXiv:1902.08153*, 2019.
- [11] Angela Fan, Edouard Grave, and Armand Joulin. Reducing transformer depth on demand with structured dropout. *arXiv preprint arXiv:1909.11556*, 2019.
- [12] Angela Fan, Pierre Stock, Benjamin Graham, Edouard Grave, Remi Gribonval, Herve Jegou, and Armand Joulin. Training with quantization noise for extreme fixed-point compression. *arXiv preprint arXiv:2004.07320*, 2020.
- [13] Jonathan Frankle and Michael Carbin. The lottery ticket hypothesis: Finding sparse, trainable neural networks. *arXiv preprint arXiv:1803.03635*, 2018.
- [14] Trevor Gale, Erich Elsen, and Sara Hooker. The state of sparsity in deep neural networks. *arXiv preprint arXiv:1902.09574*, 2019.
- [15] Song Han, Huizi Mao, and William J Dally. Deep compression: Compressing deep neural networks with pruning, trained quantization and huffman coding. *International Conference on Learning Representations*, 2016.
- [16] Yihui He, Ji Lin, Zhijian Liu, Hanrui Wang, Li-Jia Li, and Song Han. Amc: Automl for model compression and acceleration on mobile devices. In *Proceedings of the European Conference on Computer Vision (ECCV)*, pages 784–800, 2018.
- [17] Sepp Hochreiter and Jürgen Schmidhuber. Long short-term memory. *Neural computation*, 9(8):1735–1780, 1997.
- [18] Zehao Huang and Naiyan Wang. Data-driven sparse structure selection for deep neural networks. In *Proceedings of the European conference on computer vision (ECCV)*, pages 304–320, 2018.
- [19] Forrest N Iandola, Albert E Shaw, Ravi Krishna, and Kurt W Keutzer. SqueezeBERT: What can computer vision teach NLP about efficient neural networks? *arXiv preprint arXiv:2006.11316*, 2020.
- [20] Shankar Iyer, Nikhil Dandekar, and Kornl Csernai. First quora dataset release: Question pairs, 2017. URL <https://data.quora.com/First-Quora-Dataset-Release-Question-Pairs>, 2017.
- [21] Xiaoqi Jiao, Yichun Yin, Lifeng Shang, Xin Jiang, Xiao Chen, Linlin Li, Fang Wang, and Qun Liu. TinyBERT: Distilling BERT for natural language understanding. *arXiv preprint arXiv:1909.10351*, 2019.
- [22] Nikita Kitaev, Łukasz Kaiser, and Anselm Levskaya. Reformer: The efficient transformer. *arXiv preprint arXiv:2001.04451*, 2020.
- [23] Zhenzhong Lan, Mingda Chen, Sebastian Goodman, Kevin Gimpel, Piyush Sharma, and Radu Soricut. ALBERT: A lite bert for self-supervised learning of language representations. In *International Conference on Learning Representations*, 2019.
- [24] Namhoon Lee, Thalaiyasingam Ajanthan, and Philip HS Torr. Snip: Single-shot network pruning based on connection sensitivity. *arXiv preprint arXiv:1810.02340*, 2018.
- [25] Shaohui Lin, Rongrong Ji, Yuchao Li, Yongjian Wu, Feiyue Huang, and Baochang Zhang. Accelerating convolutional networks via global & dynamic filter pruning. In *IJCAI*, pages 2425–2432, 2018.
- [26] Jian-Hao Luo, Jianxin Wu, and Weiyao Lin. Thinet: A filter level pruning method for deep neural network compression. In *Proceedings of the IEEE international conference on computer vision*, pages 5058–5066, 2017.
- [27] Paul Michel, Omer Levy, and Graham Neubig. Are sixteen heads really better than one? *arXiv preprint arXiv:1905.10650*, 2019.

- [28] Sharan Narang, Eric Undersander, and Gregory Diamos. Block-sparse recurrent neural networks. *arXiv preprint arXiv:1711.02782*, 2017.
- [29] Sejun Park, Jaeho Lee, Sangwoo Mo, and Jinwoo Shin. Lookahead: a far-sighted alternative of magnitude-based pruning. *arXiv preprint arXiv:2002.04809*, 2020.
- [30] Adam Paszke, Sam Gross, Francisco Massa, Adam Lerer, James Bradbury, Gregory Chanan, Trevor Killeen, Zeming Lin, Natalia Gimelshein, Luca Antiga, Alban Desmaison, Andreas Kopf, Edward Yang, Zachary DeVito, Martin Raison, Alykhan Tejani, Sasank Chilamkurthy, Benoit Steiner, Lu Fang, Junjie Bai, and Soumith Chintala. Pytorch: An imperative style, high-performance deep learning library. In H. Wallach, H. Larochelle, A. Beygelzimer, F. d'Alché-Buc, E. Fox, and R. Garnett, editors, *Advances in Neural Information Processing Systems 32*, pages 8024–8035, 2019.
- [31] Sai Prasanna, Anna Rogers, and Anna Rumshisky. When BERT plays the lottery, all tickets are winning. *arXiv preprint arXiv:2005.00561*, 2020.
- [32] Colin Raffel, Noam Shazeer, Adam Roberts, Katherine Lee, Sharan Narang, Michael Matena, Yanqi Zhou, Wei Li, and Peter J Liu. Exploring the limits of transfer learning with a unified text-to-text transformer. *arXiv preprint arXiv:1910.10683*, 2019.
- [33] Pranav Rajpurkar, Jian Zhang, Konstantin Lopyrev, and Percy Liang. Squad: 100,000+ questions for machine comprehension of text. *arXiv preprint arXiv:1606.05250*, 2016.
- [34] Hassan Sajjad, Fahim Dalvi, Nadir Durrani, and Preslav Nakov. Poor man’s BERT: Smaller and faster transformer models. *arXiv preprint arXiv:2004.03844*, 2020.
- [35] Victor Sanh, Lysandre Debut, Julien Chaumond, and Thomas Wolf. DistilBERT, a distilled version of bert: smaller, faster, cheaper and lighter. *arXiv preprint arXiv:1910.01108*, 2019.
- [36] Victor Sanh, Thomas Wolf, and Alexander M Rush. Movement pruning: Adaptive sparsity by fine-tuning. *arXiv preprint arXiv:2005.07683*, 2020.
- [37] Sheng Shen, Zhen Dong, Jiayu Ye, Linjian Ma, Zhewei Yao, Amir Gholami, Michael W Mahoney, and Kurt Keutzer. Q-BERT: Hessian based ultra low precision quantization of bert. In *AAAI*, pages 8815–8821, 2020.
- [38] Mohammad Shoeybi, Mostofa Patwary, Raul Puri, Patrick LeGresley, Jared Casper, and Bryan Catanzaro. Megatron-LM: Training multi-billion parameter language models using gpu model parallelism. *arXiv preprint arXiv:1909.08053*, 2019.
- [39] Siqi Sun, Yu Cheng, Zhe Gan, and Jingjing Liu. Patient knowledge distillation for bert model compression. *arXiv preprint arXiv:1908.09355*, 2019.
- [40] Zhiqing Sun, Hongkun Yu, Xiaodan Song, Renjie Liu, Yiming Yang, and Denny Zhou. MobileBERT: a compact task-agnostic BERT for resource-limited devices. *arXiv preprint arXiv:2004.02984*, 2020.
- [41] Raphael Tang, Yao Lu, Linqing Liu, Lili Mou, Olga Vechtomova, and Jimmy Lin. Distilling task-specific knowledge from BERT into simple neural networks. *arXiv preprint arXiv:1903.12136*, 2019.
- [42] Philippe Tillet, HT Kung, and David Cox. Triton: an intermediate language and compiler for tiled neural network computations. In *Proceedings of the 3rd ACM SIGPLAN International Workshop on Machine Learning and Programming Languages*, pages 10–19, 2019.
- [43] Ashish Vaswani, Noam Shazeer, Niki Parmar, Jakob Uszkoreit, Llion Jones, Aidan N Gomez, Łukasz Kaiser, and Illia Polosukhin. Attention is all you need. In *Advances in neural information processing systems*, pages 5998–6008, 2017.

- [44] Hanrui Wang, Zhekai Zhang, and Song Han. Spatten: Efficient sparse attention architecture with cascade token and head pruning. *arXiv preprint arXiv:2012.09852*, 2020.
- [45] Sinong Wang, Belinda Li, Madian Khabsa, Han Fang, and Hao Ma. Linformer: Self-attention with linear complexity. *arXiv preprint arXiv:2006.04768*, 2020.
- [46] Ziheng Wang, Jeremy Wohlwend, and Tao Lei. Structured pruning of large language models. *arXiv preprint arXiv:1910.04732*, 2019.
- [47] Wei Wen, Yuxiong He, Samyam Rajbhandari, Minjia Zhang, Wenhan Wang, Fang Liu, Bin Hu, Yiran Chen, and Hai Li. Learning intrinsic sparse structures within long short-term memory. *arXiv preprint arXiv:1709.05027*, 2017.
- [48] Adina Williams, Nikita Nangia, and Samuel R Bowman. A broad-coverage challenge corpus for sentence understanding through inference. *arXiv preprint arXiv:1704.05426*, 2017.
- [49] Xia Xiao, Zigeng Wang, and Sanguthevar Rajasekaran. Autoprune: Automatic network pruning by regularizing auxiliary parameters. In *Advances in Neural Information Processing Systems*, pages 13681–13691, 2019.
- [50] Haonan Yu, Sergey Edunov, Yuandong Tian, and Ari S Morcos. Playing the lottery with rewards and multiple languages: lottery tickets in rl and nlp. *arXiv preprint arXiv:1906.02768*, 2019.
- [51] Ruichi Yu, Ang Li, Chun-Fu Chen, Jui-Hsin Lai, Vlad I Morariu, Xintong Han, Mingfei Gao, Ching-Yung Lin, and Larry S Davis. Nisp: Pruning networks using neuron importance score propagation. In *Proceedings of the IEEE Conference on Computer Vision and Pattern Recognition*, pages 9194–9203, 2018.
- [52] Shixing Yu, Zhewei Yao, Amir Gholami, Zhen Dong, Michael W Mahoney, and Kurt Keutzer. Hessian-aware pruning and optimal neural implant. *arXiv preprint arXiv:2101.08940*, 2021.
- [53] Ali Hadi Zadeh, Isak Edo, Omar Mohamed Awad, and Andreas Moshovos. Gobo: Quantizing attention-based nlp models for low latency and energy efficient inference. In *2020 53rd Annual IEEE/ACM International Symposium on Microarchitecture (MICRO)*, pages 811–824. IEEE, 2020.
- [54] Ofir Zafrir, Guy Boudoukh, Peter Izsak, and Moshe Wasserblat. Q8BERT: Quantized 8bit bert. *arXiv preprint arXiv:1910.06188*, 2019.
- [55] Wei Zhang, Lu Hou, Yichun Yin, Lifeng Shang, Xiao Chen, Xin Jiang, and Qun Liu. Ternarybert: Distillation-aware ultra-low bit bert. *arXiv preprint arXiv:2009.12812*, 2020.
- [56] Chenglong Zhao, Bingbing Ni, Jian Zhang, Qiwei Zhao, Wenjun Zhang, and Qi Tian. Variational convolutional neural network pruning. In *Proceedings of the IEEE Conference on Computer Vision and Pattern Recognition*, pages 2780–2789, 2019.
- [57] Mengjie Zhao, Tao Lin, Fei Mi, Martin Jaggi, and Hinrich Schütze. Masking as an efficient alternative to finetuning for pretrained language models. *arXiv preprint arXiv:2004.12406*, 2020.
- [58] Michael Zhu and Suyog Gupta. To prune, or not to prune: exploring the efficacy of pruning for model compression. *arXiv preprint arXiv:1710.01878*, 2017.

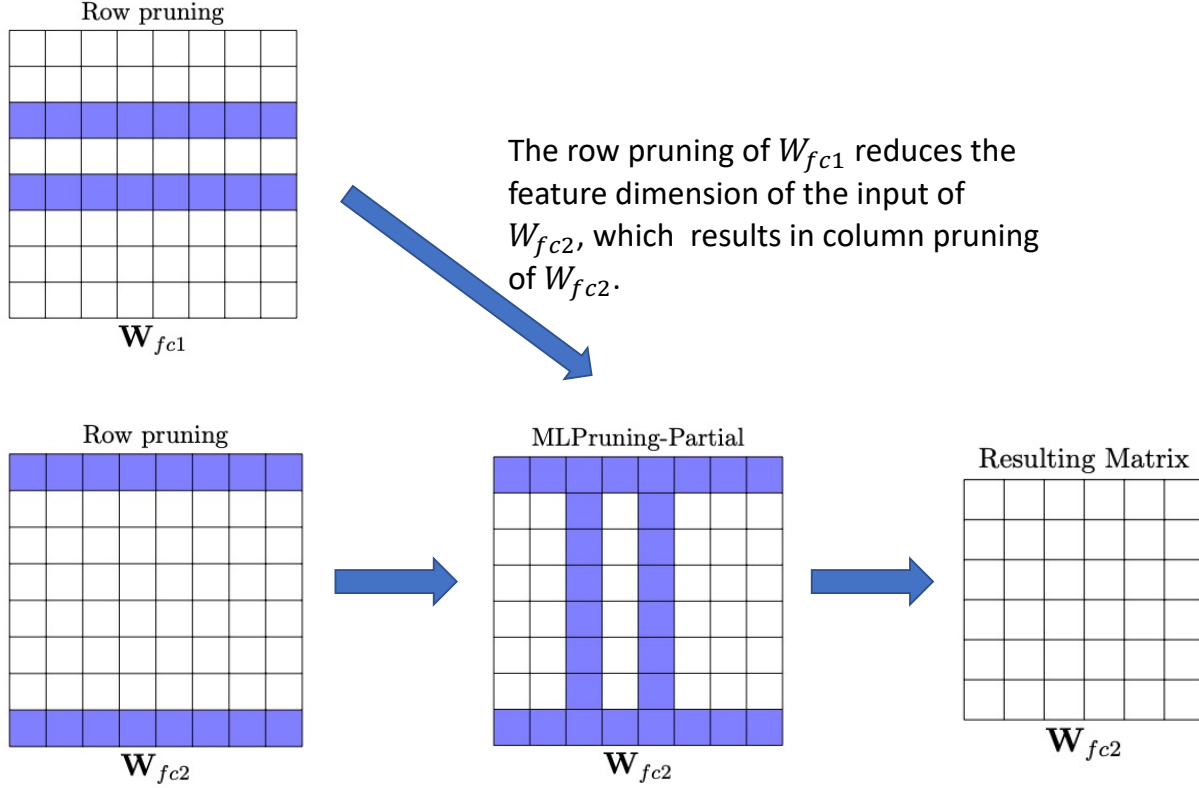


Figure B.1: Illustration of MLPruning-Partial. Blue colored cells represent the pruned weights.

A How to Mask

When we apply HPruning, RPruning, and BPruning, the shape of \mathbf{S}/\mathbf{M} is not the same as \mathbf{W} . Here, we use BERT_{base} as an example to discuss, for different pruning methods, what the shape of \mathbf{S} is (\mathbf{M} has the same shape as \mathbf{S}), and how we apply \mathbf{M} to mask \mathbf{W} .

For HPruning, since there are twelve heads, \mathbf{S} is in \mathbb{R}^{12} . When we apply \mathbf{M} to mask \mathbf{W} , we basically make the i -th head pruned if $\mathbf{M}[i] = 0$.

For RPruning, suppose there are d rows in \mathbf{W} , then \mathbf{S} is in \mathbb{R}^d . When we apply \mathbf{M} to mask \mathbf{W} , we basically make the i -th row pruned if $\mathbf{M}[i] = 0$.

For BPruning, suppose $\mathbf{W} \in \mathbb{R}^{d_1 \times d_2}$, and the block size is $a \times b$, so that there are $c \times d = \frac{d_1}{a} \times \frac{d_2}{b}$ blocks. Then the shape of $\mathbf{S} \in \mathbb{R}^{c \times d}$. When we apply \mathbf{M} to mask \mathbf{W} , we basically make the block at i -th row and j -th column pruned if $\mathbf{M}[i, j] = 0$.

B Illustration of MLPruning-Partial and MLPruning

The illustrations of MLPruning-Partial and MLPruning are shown in Figure B.1 and Figure B.2, respectively.

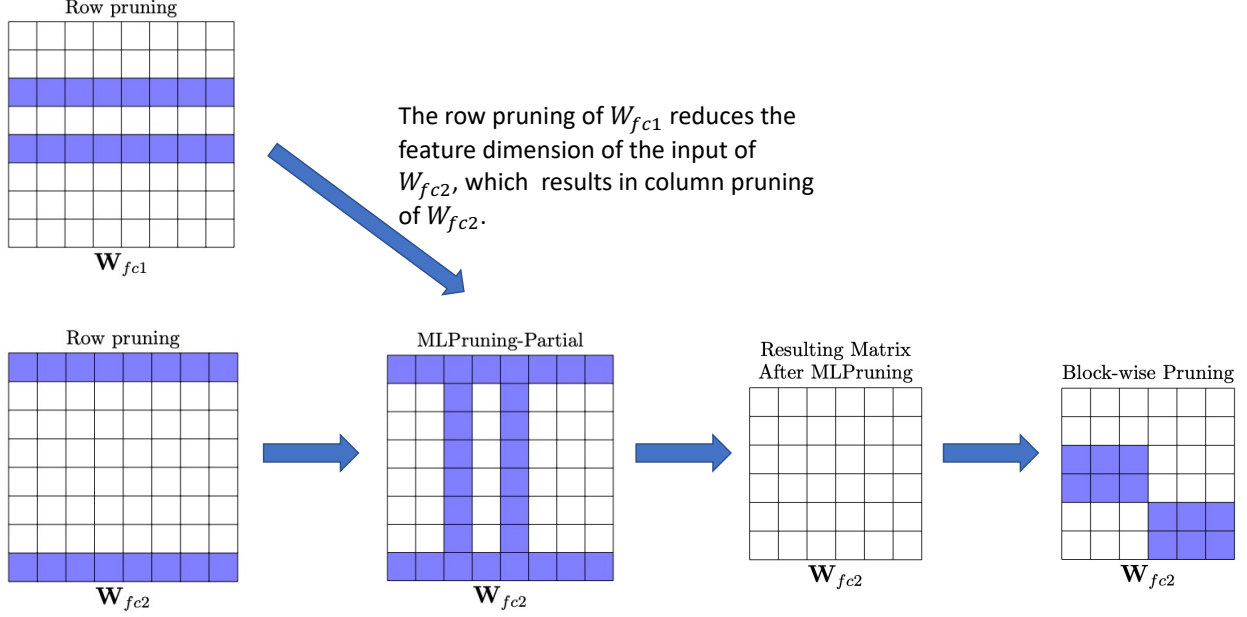


Figure B.2: Pipeline illustration of MLPruning. Blue colored cells represent the pruned weights.

C Training Details

QQP/MNLI. The temperature parameter used to compute \mathcal{L}_{DS} is 2 (i.e., the temperature used to compute the KL divergence loss between the teacher model and the student model). For BPruning, since it has fewer heads in MHA than the full model, we use the model after MLPruning-Partial as the teacher model to do the knowledge distillation. In § 5, we show that using the full model (in this case, we need to remove the \mathcal{L}_{MHA}) gets worse results, as compared to our method.

For our adaptive regularization, we choose $\lambda_{max} = 20000$, and $\lambda_{min} = 50$ for QQP/MNLI. Meanwhile, for all experiments, we fine-tune the pre-trained model for 20 epochs. We use a batch size 32 and a sequence 128 for QQP/MNLI, and we use 11000/12000 warmup steps (about 1 epoch) for learning rate. We use a learning rate of $3e-5$ ($1e-2$) for the original weights (for pruning-rated parameters, i.e., \mathbf{S} and σ) for QQP/MNLI. The initialization of \mathbf{S}/σ is $\mathbf{0}/10$. Note that all the models are trained using FP16 with PyTorch on a Titan RTX GPU (locally) or A100 GPU(AWS p4 instance).

SQuAD. For our adaptive regularization, we choose $\lambda_{max} = 10000$, and $\lambda_{min} = 50$. Meanwhile, for all experiments, we fine-tune the pre-trained model for 10 epochs. We use a batch size 12 and a sequence 384, and we use 7300 warmup steps (about 1 epoch) for the learning rate. For pruning rated parameters (\mathbf{S} and

σ), we use a learning rate of 1e-2. We tune the learning rate from {3e-5, 4e-5, 5e-5} for weight parameters, and tune the temperature used to compute \mathcal{L}_{DS} from {10, 20} for MLPruning-Partial (from {5, 10} for BPruning). We report the best result from those six hyperparameters. The initialization of \mathbf{S}/σ is $\mathbf{0}/10$. Note that all the models are trained using FP16 with PyTorch on a Titan RTX GPU (locally) or A100 GPU(AWS p4 instance).

Hardware Deployment. Our inference performances are collected on top of an NVIDIA T4 GPU (AWS g4dn.xlarge instance), which has 16 GB GDDR6 memory and a 70W maximum power limit. For each inference throughput result, we first run the inference experiment 10 times as a warm-up. Then we run the inference 100 times, and we report the mean performance.

D More BPruning Results

Here, we report more BPruning results on QQP, MNLI, and SQuAD. In particular, the BPruning results with block size 4x4 and 8x8 are also shown in Table D.1. Note that, although Triton cannot support sparse-dense MatMul for block size smaller than 16x16, those block sizes can still get significant speedup gain on other accelerators, e.g., CPU and FPGA. Supporting all hardware is beyond the scope of our work.

E Brute Force Results

Here, we report all the results using brute-force (grid-search) method for the combination of HPruning and RPruning. Note that for different layers, the head pruning ratio and the row pruning are the same. During training, we are following the strategy in [36, Eq. 5] to warm up and cool down the pruning threshold. We directly use the hyperparameters provided by [36] to train the model on QQP/MNLI.⁵

The remaining weights after pruning are provided in Table E.1, and the final accuracy of QQP/MNLI are shown in Table E.2/E.3.

F Limitations and Future Work

We believe it is critical for every work to state clearly its limitations, especially in this area. An important limitation is that for the second step of our two-step pipeline pruning algorithm, we still need to fully retrain the model. This adds some computational overhead. (Although, this is currently common for model compression methods.) It is an interesting direction to find a more efficient fine-tuning algorithm for the second step. Another limitation is that in this work we solely focused on BERT models, but it would be interesting to see how MLPruning would perform for other NLP problems, e.g., neural machine translation. Finally, in this work, we only explore the effect of MLPruning on static inference (i.e., the model architecture is fixed during inference). However, the dynamical inference is another interesting direction that can be studied.

⁵The parameters are provided by authors at https://docs.google.com/spreadsheets/d/17JgRq_OFFTniUrz6BZWW_87DjFkKXpI1kYDSsseT_7g/edit#gid=444654759. For MNLI, we increase the training epochs to 10, increase the initial_warmup to 2, and increase the final_warmup to 3.

Table D.1: Performance of MLPruning on different datasets. For the last performance column, we report the mean of F1 and accuracy on QQP, the accuracy for MNLI-M/MNLI-MM on MNLI, and exact match (EM) and F1 on SQuAD.

Dataset	Block Size	Remaining Weight %	Block Density %						Performance
			W_q	W_k	W_v	W_o	W_{fc1}	W_{fc2}	
QQP	4x4	35.51	96.17	99.02	52.45	34.22	88.77	75.76	89.36
	4x4	22.97	75.69	77.90	34.42	42.02	37.46	68.93	89.27
	4x4	14.13	59.45	59.63	38.54	59.19	10.66	26.34	89.10
	4x4	11.95	56.30	56.31	42.48	59.57	4.40	12.63	88.75
	8x8	35.54	94.36	98.85	57.32	33.17	79.02	98.36	89.22
	8x8	22.80	81.68	91.18	45.08	53.88	38.60	36.04	89.10
	8x8	18.57	73.20	73.62	39.82	66.71	25.31	26.66	89.08
	8x8	14.15	59.37	59.46	49.53	65.22	8.44	21.35	89.02
	8x8	10.90	56.57	44.30	30.99	61.41	4.79	13.40	88.61
	16x16	34.76	90.48	95.28	59.98	33.45	75.81	97.23	89.09
	16x16	18.55	73.81	75.33	41.03	65.97	24.28	26.33	89.02
	16x16	14.19	59.73	59.98	50.26	65.17	8.45	20.39	89.01
	16x16	11.97	56.33	56.35	41.18	60.30	4.49	13.49	88.46
	32x32	34.75	87.97	95.58	64.42	38.35	83.12	72.88	88.99
	32x32	18.73	73.36	74.91	65.17	64.70	21.42	19.43	89.01
	32x32	14.28	71.14	62.27	51.40	64.70	6.39	16.01	88.56
MNLI	4x4	38.79	98.84	99.86	63.23	40.09	95.40	62.94	83.21/83.77
	4x4	25.08	80.41	73.11	50.22	55.01	39.02	38.42	82.86/83.18
	4x4	20.25	68.96	69.09	48.15	56.32	21.24	26.78	81.97/82.95
	4x4	15.83	67.40	67.42	45.74	69.03	4.75	5.51	81.80/82.48
	8x8	38.29	99.22	99.77	63.01	41.64	95.02	57.77	82.86/83.44
	8x8	25.10	72.73	74.76	50.53	56.17	37.73	43.10	82.50/83.01
	8x8	20.27	69.14	69.29	47.37	69.96	19.42	24.02	81.85/82.67
	8x8	15.68	67.38	67.43	46.08	67.40	3.70	5.96	81.17/81.77
	16x16	37.74	99.78	99.69	63.76	52.57	89.29	54.48	82.57/83.12
	16x16	25.15	72.17	73.54	49.19	55.36	36.21	47.51	82.40/82.96
	16x16	20.31	71.01	71.75	47.44	69.93	18.28	23.06	81.71/82.59
	16x16	15.91	68.28	68.31	46.03	69.31	4.52	5.04	80.98/81.49
	32x32	36.89	92.23	99.77	59.53	53.61	88.23	53.35	82.51/83.19
	32x32	25.25	73.66	74.98	46.76	54.33	36.06	48.10	82.42/82.75
	32x32	20.40	71.00	71.67	47.45	69.93	18.34	23.05	81.71/82.49
	32x32	20.40	71.00	71.67	47.45	69.93	18.34	23.05	81.71/82.49
SQuAD	16x16	48.30	95.52	98.15	78.97	71.69	81.94	66.84	80.83/88.11
	16x16	36.84	95.60	99.17	88.66	79.80	40.46	36.08	80.17/87.60
	16x16	31.23	94.77	99.46	98.99	84.27	17.90	21.24	78.30/86.46
	16x16	25.21	92.74	91.55	90.58	82.20	5.98	5.92	77.81/86.10
	16x16	20.97	48.53	80.38	80.53	90.58	4.85	4.22	75.70/84.63
	32x32	45.13	93.51	97.25	77.32	70.52	70.20	62.50	80.56/87.85
	32x32	36.60	96.81	99.32	81.31	78.52	40.33	36.99	79.72/87.38
	32x32	25.32	94.52	92.53	92.35	81.39	5.72	5.34	77.00/85.79
	32x32	20.47	50.17	80.59	80.68	79.93	4.94	4.26	75.49/84.45
	32x32	20.47	50.17	80.59	80.68	79.93	4.94	4.26	75.49/84.45

Table E.1: Remaining parameters when using brute-force (grid-search) method to find the combination of HPruning and RPruning. Here, the first column means the remaining head number, and the first row means the remaining FC weight parameters. The numbers reported here are the percents of remaining parameters. Note that for different layers, the pruning ratios are uniform and fixed.

	100%	90%	80%	70%	60%	50%	40%	30%	20%	10%
12	100.0	90.32	81.33	73.00	65.34	58.37	52.03	46.37	41.37	37.04
11	97.22	87.54	78.55	70.22	62.56	55.59	49.25	43.59	38.59	34.27
10	94.45	84.77	75.77	67.45	59.79	52.82	46.47	40.81	35.82	31.49
9	91.67	81.99	73.00	64.67	57.01	50.04	43.70	38.04	33.04	28.71
8	88.89	79.21	70.22	61.89	54.23	47.26	40.92	35.26	30.26	25.94
7	86.12	76.44	67.44	59.12	51.46	44.49	38.14	32.48	27.49	23.16
6	83.34	73.66	64.76	56.34	48.68	41.71	35.37	29.71	24.71	20.38
5	80.56	70.88	61.89	53.56	45.90	38.93	32.59	26.93	21.94	17.61
4	77.79	68.11	59.11	50.79	43.13	36.16	29.81	24.15	19.16	14.83
3	75.01	65.33	56.34	48.01	40.35	33.38	27.04	21.38	16.38	12.05
2	72.23	62.55	53.56	45.23	37.57	30.60	24.26	18.60	13.61	9.280
1	69.46	59.78	50.78	42.46	34.80	27.83	21.48	15.82	10.83	6.50

Table E.2: Using brute-force (grid-search) method to find the combination of HPruning and RPruning on QQP. The reported numbers are the mean of F1 and accuracy. Here, the first column means the remaining head number, and the first row means the remaining FC weight parameters. All experiments are using distillation as we used in the main text. Note that for different layers, the pruning ratios are uniform and fixed.

	100%	90%	80%	70%	60%	50%	40%	30%	20%	10%
12	—	89.89	89.69	89.34	89.01	89.03	88.98	88.77	88.61	88.46
11	89.88	89.56	89.65	89.57	89.27	88.94	88.89	88.80	88.62	88.39
10	89.95	89.51	89.31	89.31	89.27	88.94	88.77	88.70	88.57	88.39
9	89.84	89.58	89.37	89.12	89.02	89.09	88.79	88.56	88.29	88.33
8	89.55	89.41	89.60	89.32	88.96	88.64	88.64	88.42	88.29	88.13
7	89.32	89.23	89.38	89.10	88.84	88.63	88.27	88.27	88.07	87.95
6	89.31	89.11	89.14	88.97	88.77	88.50	88.29	87.84	88.04	87.71
5	89.24	89.02	88.79	88.77	88.45	88.11	87.87	87.75	87.64	87.48
4	89.21	88.95	88.84	88.70	88.02	87.99	87.63	87.64	87.27	87.02
3	88.79	88.44	88.47	88.06	87.88	87.34	87.31	87.06	86.67	86.12
2	88.53	88.19	87.42	87.45	87.18	86.72	86.10	86.42	85.51	84.76
1	87.01	86.56	86.39	86.07	85.68	85.16	84.88	84.54	84.39	83.63

Table E.3: Using brute-force (grid-search) method to find the combination of HPruning and RPruning on MNLI. The reported numbers are the accuracy for MNLI-M and MNLI-MM. Here, the first column means the remaining head number, and the first row means the remaining FC weight parameters. All experiments are using distillation as we used in the main text. Note that for different layers, the pruning ratios are uniform and fixed.

	100%	90%	80%	70%	60%	50%	40%	30%	20%	10%
12	–	84.92/84.93	84.71/84.64	84.01/84.80	84.00/84.37	83.77/84.27	83.28/83.65	82.87/83.65	82.30/82.99	81.74/82.57
11	85.20/85.44	84.81/85.04	84.72/84.73	84.10/84.68	83.78/84.19	83.37/84.03	83.49/83.82	82.86/83.48	82.24/82.75	81.78/82.29
10	84.90/85.10	84.54/84.76	84.44/84.84	84.06/84.52	83.82/84.08	83.56/84.08	82.78/83.50	82.64/83.22	82.06/82.95	81.58/82.41
9	84.81/85.06	84.32/84.86	84.16/84.78	83.86/84.32	83.32/84.05	83.17/83.84	82.78/83.27	82.33/82.80	81.66/82.27	80.98/82.18
8	84.41/85.10	84.25/84.44	83.73/84.10	83.68/84.06	83.18/83.71	82.93/83.19	82.54/83.10	81.74/82.56	81.38/82.15	81.05/82.02
7	84.34/84.63	84.03/84.60	83.36/83.93	83.61/84.05	82.81/83.69	82.52/83.29	82.25/82.57	81.62/82.27	81.31/82.01	80.87/81.50
6	83.95/84.42	83.76/83.88	83.41/84.21	83.12/83.90	82.74/83.20	82.34/83.09	81.82/82.89	81.48/81.98	81.01/81.54	80.48/80.99
5	83.91/84.01	83.03/83.59	83.05/83.13	82.67/83.79	82.67/83.09	81.93/82.57	81.27/82.39	81.14/81.80	80.82/81.56	80.30/80.75
4	82.86/83.98	82.90/83.39	82.51/83.41	82.42/82.83	81.60/82.32	81.28/81.94	81.17/81.88	80.79/81.12	80.17/81.04	79.65/80.23
3	82.98/83.16	82.66/82.84	81.95/82.33	81.99/82.08	81.50/82.15	80.91/82.00	80.26/81.12	80.23/80.18	80.22/80.66	79.38/79.52
2	81.07/81.28	81.43/81.09	80.88/81.04	80.41/80.80	80.63/80.64	80.07/80.71	79.83/79.86	78.56/79.54	77.94/78.37	78.43/79.00
1	79.08/79.02	77.94/78.21	77.15/77.51	77.21/77.59	76.54/76.83	76.58/76.69	75.93/77.10	75.21/76.05	74.30/75.56	73.65/73.75